

Temperature-Dependent Photoluminescence of CdSe-Core CdS/CdZnS/ZnS-Multishell Quantum Dots

Pengtao Jing,^{†,‡} Jinju Zheng,^{†,‡} Micho Ikezawa,[§] Xueyan Liu,[†] Shaozhe Lv,[†] Xianggui Kong,[†] Jialong Zhao,^{*,†} and Yasuaki Masumoto^{*,§}

Key Laboratory of Excited State Processes, Changchun Institute of Optics, Fine Mechanics and Physics, Chinese Academy of Sciences, 3888 Eastern South Lake Road, Changchun 130033, China, Graduate School of Chinese Academy of Sciences, Beijing 100039, China, and Institute of Physics, University of Tsukuba, Tsukuba, Ibaraki 305-8571, Japan

Received: March 8, 2009; Revised Manuscript Received: June 22, 2009

The photoluminescence (PL) spectra of CdSe-core CdS/CdZnS/ZnS-multishell quantum dots (QDs) were studied to understand the radiative and nonradiative relaxation processes in the temperature range from 80 to 360 K. The mechanism of temperature-dependent nonradiative relaxation processes in the CdSe QDs with changing the shell structures was found to evolve from thermal activation of carrier trapping by surface defects/traps in CdSe core QDs to the multiple longitudinal-optical (LO) phonon-assisted thermal escape of carriers in the core/shell QDs. An increase in PL intensity with increasing temperature was clearly observed in the core/shell QDs with a thick CdS monoshell and a CdS/ZnCdS/ZnS multishell. The PL enhancement was considered to come from delocalization of charge carriers localized at the CdSe/CdS interface with the potential depth of ~ 30 meV. The experimental results indicated that the improvement of PL quantum efficiency in CdSe-core CdS/CdZnS/ZnS-multishell QDs could be understood in terms of the reduction of nonradiative recombination centers at the interfaces and on the surface of the multishell, as well as the confinement of electrons and holes into the QDs by an outer ZnS shell.

Introduction

Semiconductor quantum dots (QDs) with a size-tunable bandgap have been widely applied in light-emitting diodes (LEDs),^{1–8} photovoltaic cells,^{9,10} and biological labels.¹¹ CdSe QDs with high-photoluminescence (PL) quantum yield (QY) and good photostability were obtained by growing a monoshell (CdS or ZnS) on CdSe cores.¹² Recently, the PL QY up to 85% was reached by using a multishell (CdS/CdZnS/ZnS), which integrated the advantages of a small lattice mismatch between the CdSe core and CdS shell and a high-energy barrier between the CdSe core and the outer ZnS shell.¹³ More recently, we found that the multishell structure could efficiently suppress the static quenching that the number of emitting centers was decreased by hole-transporting materials (HTMs), compared with the core/monoshell QDs.¹⁴ By now CdSe QD-LEDs fabricated by using the core/multishell QDs have shown efficient electroluminescence.^{4–6} However, further improvement of the performance for these QD-based devices depends not only on higher PL QY of QDs but also on better structures of QDs.

It is known that the PL QY of CdSe/ZnS core/shell QDs significantly decreases when a relatively thick ZnS shell is grown on CdSe cores, resulting from a large amount of defects/traps formed at the interface between the CdSe core and ZnS shell due to the large lattice mismatch and interfacial strain.^{12,13,15} These defects/traps are considered to be efficient nonradiative recombination centers that determine the PL QY of the core/

shell QDs. For the CdSe core/multishell QDs the PL QY significantly increases with growing the first layer of CdS shell and slightly decreases with growing CdZnS and ZnS shells continuously while their photostability is significantly enhanced.¹³ Therefore, it is necessary to explore whether the defects/traps are formed at the core/shell and shell/shell interfaces or the surface of CdSe-core CdS/CdZnS/ZnS-multishell QDs for further improvement of the quality of the QDs.

Temperature-dependent PL spectroscopy is often used to study the radiative and nonradiative relaxation processes, as well as exciton–phonon coupling in colloidal core and core/monoshell QDs.^{16–19} In general, the integrated PL intensity of the QDs exponentially decreases with increasing temperature because of thermal quenching. The thermal quenching behavior in the core and core/shell QDs was attributed to carrier trapping by surface defect states/traps or/and thermal escape assisted by the scattering with multiple LO phonons.^{16,17} Furthermore, the ligand shell also can influence the temperature dependence of PL intensity in QDs. Wuister et al. observed the temperature anti-quenching of PL from capped CdSe QDs due to the surface ligand restructure with increasing temperature.¹⁹ To date, no report has been given about the mechanism of nonradiative relaxation processes in CdSe-core CdS/CdZnS/ZnS-multishell QDs.

In this work, we report the temperature-dependent PL spectra of CdSe/CdS/CdZnS/ZnS core/multishell QDs, comparing those of the CdSe core, traditional CdSe/ZnS and CdSe/CdS core/monoshell QDs. The mechanism of nonradiative relaxation processes in the QDs is explored by using the temperature dependence of the PL intensity in the core/shell QDs with various shell thicknesses and structures. Furthermore, we explain the PL enhancement in CdSe/CdS(6 ML) and CdSe/multishell(6 ML) QDs with increasing temperature in terms of thermal

* To whom correspondence should be addressed. Phone: +86-431-86176029 (J.Z.); +81-29-8534248 (Y.M.). E-mail: jlzhaoqd@yahoo.com (J.Z.); shoichi@sakura.cc.tsukuba.ac.jp (Y.M.).

[†] Changchun Institute of Optics, Fine Mechanics and Physics, Chinese Academy of Sciences.

[‡] Graduate School of Chinese Academy of Sciences.

[§] University of Tsukuba.

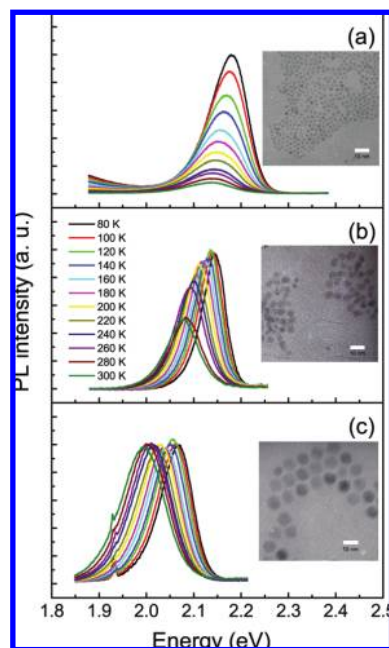


Figure 1. PL spectra of CdSe core (a), CdSe/CdS(3 ML) core/monoshell (b), and CdSe/CdS(3 ML)/CdZnS(1 ML)/ZnS(2 ML) core/multishell QDs (c) at different temperature from 80 to 300 K under excitation at 488 nm. Typical TEM images of the QDs are shown in the inset. Scale bar is 10 nm.

activation of charge carriers localized at the core(CdSe)/shell(CdS) interface.

Experimental Section

The CdSe core QDs were synthesized using standard methods.²⁰ The shell layers of ZnS, CdS, and CdS/ZnCdS/ZnS were grown onto CdSe cores by using a successive ion layer absorption and reaction (SILAR) method.¹³ The same CdSe cores with a diameter of about 3 nm were used to prepare the core/shell QDs. The shell thicknesses were determined via the comparison of the sizes of core and core/shell QDs measured by a JEM-2010 transmission electron microscope (TEM), and the shell layers were estimated on the basis of one monolayer (ML) of 0.31, 0.32, and 0.33 nm with respect to ZnS, ZnCdS, and CdS shell materials.¹³ The shell structures and dot diameters of the CdSe core/shell QDs are as follows. (A) ZnS(3 ML) and 4.8 nm, (B) CdS(3 ML) and 5.0 nm, (C) CdS(6 ML) and 7.0 nm, and (D) CdS(3 ML)/CdZnS(1 ML)/ZnS(2 ML) and 7.5 nm, respectively. The PL QYs of these QD samples after twice washing were determined to be about 40%, 63%, 47%, and 70%, respectively. The QDs were dispersed in poly(methyl methacrylate) (PMMA, molecular weight = 15 000) as a matrix and were then dropped on silicon wafer substrates. The molar ratio of dots/polymer is about 10^{-5} to avoid aggregation of QDs which induces the possibility of Förster energy transfer between differently sized QDs. The samples were excited by the 488 nm line of an Ar⁺ laser. The laser beam was focused onto the samples by a magnification microscope objective (10×, N.A. = 0.25). The laser spot was about 100 μm in diameter. The PL was dispersed by a monochromator and detected by a Jobin-Yvon Si-CCD. The samples were mounted in a micro-objective cryostat with a controllable temperature range from 80 to 360 K.

Results and Discussion

Figure 1 shows the temperature-dependent PL spectra of CdSe core, CdSe/CdS core/shell(3 ML), and CdSe/CdS/CdZnS/ZnS

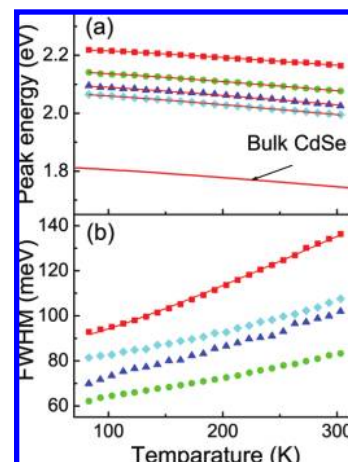


Figure 2. Temperature dependence of emission peak energy (a) and FWHM (b) of CdSe core/shell QDs with different shell structures of ZnS (3 ML) (red squares), CdS (3 ML) (green circles), CdS (6 ML) (blue triangles), and multishell (6 ML) (cyan diamonds), respectively. Solid lines represent the fitting curves. The temperature dependence of energy band gap for bulk CdSe is also plotted in (a).

core/multishell(6 ML) QDs recorded in the temperature range from 80 to 300 K. As seen in Figure 1a, the PL intensity of the core QDs quickly decreases when temperature increases. This means that there are a large amount of the nonradiative traps on the surface of the core QDs, causing strong thermal quenching. In contrast, the PL intensity of CdSe/CdS core/shell(3 ML) QDs slowly decreases with increasing temperature, as seen in Figure 1b. As a result, the surface nonradiative relaxation centers are efficiently passivated by the growth of a monoshell. Further, as shown in Figure 1c, the PL intensity of the CdSe/CdS/CdZnS/ZnS core/multishell QDs is almost kept constant when temperature changes from 80 to 300 K. This suggests that the nonradiative recombination is significantly suppressed in the multishell coated QDs. Furthermore, a long PL tail of the CdSe core QDs at the low-energy side is considered to come from the surface states or defect states.²¹ This long tail is absent in the core/shell QDs with a CdS shell(3 ML) and a CdS/CdZnS/ZnS multishell, indicating that the surface defect states are efficiently passivated by using mono- or multishells. It is also noted that the peak energies of PL bands for the core, core/monoshell, and core/multishell QDs shift to the red and their full widths at the half-maximum (FWHM) broaden with increasing temperature.

The temperature dependence of the PL peak energies for CdSe core/shell QDs with different shell structures is shown in Figure 2a. The red-shift of the PL peak wavelength for a semiconductor reflects shrink of the energy bandgap with increasing temperature due to the lattice deformation potential and exciton–phonon coupling.^{22,23} The experimental data can be fitted by an empirical Varshni relation^{16–18}

$$E_g(T) = E_{g0} - \alpha \frac{T^2}{T + \beta} \quad (1)$$

where E_{g0} is the energy gap at 0 K, α is the temperature coefficient, β is a fitting parameter that is close to the Debye temperature. The values of α and β for these core/shell QDs are listed in Table 1. The data are similar to those of bulk CdSe material ($\alpha = 3.7 \times 10^{-4}$ eV/K, $\beta = 150$ K).¹⁸ This indicates that the dominant emissions in the CdSe core/shell QDs with

TABLE 1: Fitting parameters of E_{g0} , α , and β

sample	E_{g0} (eV)	α (10^{-4} eV/K)	β (K)
CdSe/ZnS (3 ML)	2.23	3.1 ± 0.3	156.5 ± 13.1
CdSe/CdS (3 ML)	2.15	3.7 ± 0.1	155.3 ± 7.1
CdSe/CdS (6 ML)	2.11	4.0 ± 0.2	173.3 ± 19.5
CdSe/multishell (6 ML)	2.08	4.0 ± 0.8	141.3 ± 7.9
bulk ^a	1.757	3.7	150

^a Reference 18.

different shell structures come from the recombination of electrons and holes near the band edge of CdSe cores.

Figure 2b shows the PL FWHMs of CdSe core/shell QDs with different shell structures as a function of temperature. The temperature dependence of the FWHM due to exciton scattering with acoustic and LO phonons can be described by the following equation:^{16–18,24}

$$\Gamma(T) = \Gamma_{\text{inh}} + \sigma T + \Gamma_{\text{LO}}(e^{E_{\text{LO}}/k_{\text{B}}T} - 1)^{-1} \quad (2)$$

where Γ_{inh} is the inhomogeneous line width that is temperature-independent and results from fluctuation in size, shape, and composition of QDs, σ is the exciton-acoustic-phonon coupling coefficient, Γ_{LO} represents the exciton-LO-phonon coupling coefficient, and LO-phonon energy, E_{LO} , is taken as 25 meV from Raman spectra of CdSe QDs in previous reports.^{25,26} The temperature dependence of PL FWHM for CdSe/ZnS QDs can be fitted well, as shown in Figure 2b. The parameters σ and Γ_{LO} are obtained to be $78.9 \pm 2.3 \mu\text{eV/K}$ and $48.7 \pm 1.4 \text{ meV}$, respectively. The acoustic phonon dephasing rate is consistent with that of $75 \mu\text{eV/K}$ predicted in a CdSe QD of 1.5 nm in radius.²⁷ The exciton-LO phonon coupling coefficient is smaller than that of about 100 meV in bulk CdSe due to the confinement of excitonic polarization in small QDs.²⁸ Furthermore, it is found that the temperature-dependent broadening of the PL FWHMs in CdS shell (3 and 6 ML) and a multishell-coated QD deviates from that of ZnS-coated QDs despite the same core size. It is well known that the electron wave function extends into the CdS shell due to a low barrier between the conduction bands of CdSe and CdS.^{12,13} Therefore, this indicates that the PL in the CdS-shell-coated QDs may come not only from the CdSe cores but also from the interface states or emitting centers in the shells.

In order to investigate the shell effect on the nonradiative relaxation processes in QDs, we analyze the temperature dependence of integrated PL intensity. In general, the PL QY and photostability of CdSe core QDs can be improved by growing a monoshell (ZnS or CdS) with a larger bandgap to confine electrons and holes into the core.¹² The PL intensities of CdSe core and core/monoshell (3 ML) QDs with different shell materials as a function of inverse $k_{\text{B}}T$ are shown in panels a and b of Figure 3, respectively. The PL intensities are normalized to the PL one at the lowest measurement temperature of 80 K. The PL intensity of the core QDs decreases rapidly when temperature increases, compared to that of the core/monoshell (3 ML) QDs. When two typical kinds of nonradiative relaxation processes are assumed as follows. (A) Carrier trapping by surface defect states²⁹ and (B) multiple LO phonon assisted thermal escape from dots;^{16,30} the temperature dependence of the PL intensity can be described by the following equation:^{16,17}

$$I_{\text{PL}}(T) = \frac{N_0}{1 + Ae^{-E_a/k_{\text{B}}T} + B(e^{E_{\text{LO}}/k_{\text{B}}T} - 1)^{-m}} \quad (3)$$

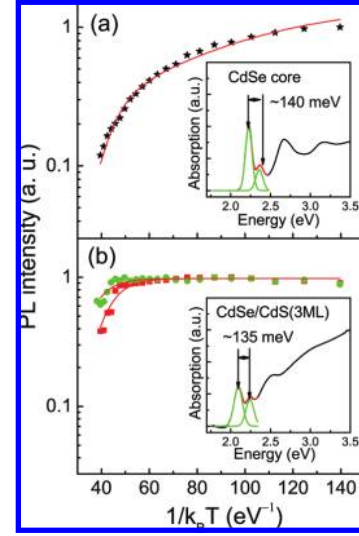


Figure 3. Integrated PL intensities of CdSe core/shell QDs with different shell structures as a function of inverse $k_{\text{B}}T$. (a) CdSe core QDs (black stars), (b) CdSe/ZnS(3 ML) (red squares), and CdSe/CdS(3 ML) (green stars) core/shell QDs. The solid lines represent fitting curves by an equation described in the text. Absorption spectra of CdSe core and CdSe/CdS(3 ML) core/shell QDs are shown in the insets of (a) and (b), respectively.

TABLE 2: Fitting Parameters of E_a , m , and ΔE

sample	E_a (meV)	m	ΔE (meV)
CdSe core	26.5 ± 1.5	5.2 ± 0.1	—
CdSe/ZnS (3 ML)	—	4.7 ± 0.2	—
CdSe/CdS (3 ML)	—	4.9 ± 0.3	—
CdSe/CdS (6 ML)	—	3.9 ± 0.2	28.1 ± 1.4
CdSe/multishell (6 ML)	—	4.6 ± 0.5	29.0 ± 1.4

where $I_{\text{PL}}(T)$ is the integrated PL intensity at temperature T , N_0 is the initial carrier population of emitting states, E_a is the activation energy of surface defect states, m is the number of LO phonons for assisted thermal escape of carriers from dots, and A and B represent the ratios of the radiative lifetime in QDs to the capture time from emitting centers by nonradiative recombination centers. The parameters E_a and m for the CdSe core, CdSe/ZnS (3 ML), and CdSe/CdS(3 ML) core/shell QDs are summarized in Table 2.

For CdSe core QDs, the activation energy of carrier trapping by surface defect states and the number of LO phonon m were determined to be $26.5 \pm 1.5 \text{ meV}$, and 5.2 ± 0.1 , respectively, as seen in Table 2. The nonradiative relaxation process with a small activation energy (10–30 meV) results in a decrease in the PL intensity of CdSe core QDs at the low temperature range.^{16,17} Furthermore, the energy of 5.2 LO phonons ($5.2 \times 25 \text{ meV} = 130 \text{ meV}$) approaches to the energy difference of about 140 meV between $1S_{3/2}$ and $2S_{3/2}$ states as seen in the absorption spectra³¹ in the inset of Figure 3a. This suggests that the thermal escape involves hole states, consistent with previous reports.^{16,17} The PL intensity of the core/shell QDs with a 3 ML CdS or ZnS shell is almost kept constant in the low-temperature range (80–200 K) and exponentially decreases with increasing temperature from 200 to 300 K, as shown in Figure 3b. On the basis of eq 3, only considering one thermally activated nonradiative recombination process, the activation energy of about 200–250 meV obtained in CdSe core/shell QDs with a 3 ML CdS or ZnS shell is larger than the energy spacing between $1S_{3/2}$ and $2S_{3/2}$ (130–140 meV, as seen in the inset of Figure 3b) and close to the exciton binding energy (EBE) of CdSe QDs with a diameter about 3–5 nm³² or an energy barrier

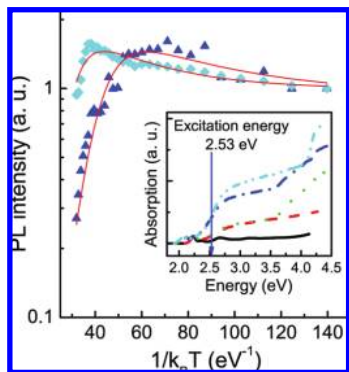


Figure 4. Integrated PL intensities of CdSe core/shell QDs with CdS (6 ML) monoshell (blue triangles) and a multishell (6 ML) (cyan diamonds) as a function of inverse $k_B T$. Inset shows absorption spectra of CdSe core (black solid line), and core/shell QDs with different shell structures of ZnS (3 ML) (red dashed line), CdS (3 ML) (green dotted line), CdS (6 ML) (blue dash-dotted line), and CdS (3 ML)/ZnS (2 ML) (cyan dash-dot-dotted line), respectively.

for conduction band offset of CdSe/CdS interface.¹² In the temperature range of 80–360 K, the thermal-induced exciton ionization or electron escape from the conduction band barrier is impossible because the thermal energy of $k_B T$ is much smaller than the EBE or the energy of the conduction band barrier. This means that the most possible nonradiative relaxation process comes from the multiple LO phonon assisted transition due to the strong polar Fröhlich coupling.³³ The temperature dependence of PL intensity for CdSe core/monoshell QDs with a thin shell (3 ML) can be fitted well by eq 3 when the carrier trapping by surface defects is ignored. The numbers of LO phonons m are determined to be 4.7 ± 0.2 and 4.9 ± 0.3 , respectively, for ZnS (3 ML) and CdS (3 ML) coated QDs, as seen in Table 2. This suggests that the multiple LO phonon assisted thermal escape from $1S_{3/2}$ to $2S_{3/2}$ dominates the PL QY in core/monoshell (3 ML) QDs as observed in previous reports.^{16,17} As seen in Figure 3b, the thermal-induced PL quenching in ZnS (3 ML) coated QDs is faster than that in CdS (3 ML) coated QDs. This indicates that there are more defects formed at the CdSe/ZnS interface due to the larger lattice mismatch between the CdSe core and ZnS shell. Generally, a large amount of interface defects are formed due to the strain relaxation when the ZnS shell thickness is more than 3 ML, reducing the PL QY, whereas the QY of CdSe/CdS core/shell QDs is still high when a thick CdS shell is grown on CdSe cores.^{12,13,16}

Figure 4 shows the temperature dependence of PL intensities in CdS (6 ML) and multishell (6 ML) coated QDs. In contrast to those in the core and core/shell (3 ML) QDs, the PL intensities of CdS monoshell (6 ML) and multishell (6 ML) coated QDs show an anti-quenching behavior with increasing temperature and reach a maximum at temperature 200 and 300 K, respectively. In these two samples, the shell thickness is reached to 6 MLs (~ 1.9 nm), doubly thicker than those of the previous core/shell QDs. In the previous discussion, the thermal quenching induced by surface defects could be reduced effectively by growing a shell (3 ML) on a CdSe core.¹² It is expected that the thick shell can greatly reduce the thermal quenching resulting from surface defects. Generally, the growth of a shell on a CdSe core is carried out at high temperature (200–260 °C) using SILAR technique.¹³ Therefore, the atom diffusion at the CdSe/CdS core/shell interface can form some traps and cause energy band fluctuation.^{35,36} The blue-shift of the emission peak, resulting from an increase of the band offset due to the atom diffusion of Zn^{2+} into $Cd_{0.5}Zn_{0.5}S$ alloy layers, has been observed

in previous reports.^{13,37} On the other hand, the energy band fluctuation induced by the lattice strain at the core/shell interface can not be ignored.^{38,39} The shift of LO phonon Raman mode observed in CdSe core/shell QDs, in contrast to CdSe cores, was attributed to the lattice strain that appeared at the core/shell interface.^{25,26} Recently, the pressure of CdS/ZnS core/shell interface was probed via the PL emission of Mn^{2+} ions doped at different positions of the QDs and demonstrated a pressure of more than 4 GPa for 7.5 MLs of ZnS.³⁹ It is assumed that the excited carriers can be localized at CdSe/CdS, CdS/CdZnS, and CdZnS/ZnS interfaces at low temperature due to the energy band fluctuation. As seen in the inset of Figure 4, the absorption of the QDs with a CdS monoshell (6 ML) or a multishell (6 ML) increases rapidly above 2.42 eV due to the absorption of the CdS shell.³⁴ The excitation light with a photon energy of 2.53 eV, slightly above the bandgap of CdS shell, can excite CdS. Thus, the emission from the localized states at the interfaces may be easily observed. These localized carriers at the core/shell and shell/shell interfaces can be thermally activated to CdSe core emitting states when temperature increases. The similar phenomena were also observed in InAs QDs embedded in InGaAs/GaAs dots in the well.^{40,41} More recently, the enhancement of the average PL lifetime with increasing temperature was observed in high-quality CdSe/CdS/ZnS QDs, which was attributed to an activated carrier detrapping process from trap states to exciton states.⁴² However, the enhancement phenomenon is not observed in a thin CdS or ZnS monoshell (3 ML) coated QDs because the surface defects may capture these localized carriers across the thin shell (~ 1 nm). Finally, a decrease in the PL intensities of these QDs at high temperature implies that the temperature-dependent nonradiative relaxation processes are also present as shown in Figure 4.

The population of the initial excited carriers at the emitting states in the CdS (6 ML) and multishell (6 ML) coated QDs is considered to come from two parts: $N_0 + N'_0 e^{-\Delta E/k_B T}$, where the first term represents the population of e/h pairs formed by direct relaxation from high-energy states to CdSe core emitting states, and the second one represents the population of charge carriers thermally activated from the interface states. The second term plays an important role in the PL intensity enhancement with increasing temperature. This would explain the PL intensity enhancement of CdS monoshell (6 ML) and multishell (6 ML) coated QDs when temperature increases. The thermal quenching becomes very small in the thick multishell (6 ML) coated QDs as seen in Figure 4, compared with that of the naked cores and a thin monoshell coated QDs. This indicates that the surface defects/traps on the core surface are excellently passivated by a multishell and the nonradiative relaxation process causing from the LO phonon assisted carrier escape is also decreased due to the thick shell as a barrier.

Further, the localization depth of carriers at the interface is estimated on the basis of the temperature dependence of PL intensity for CdS monoshell (6 ML) and multishell (6 ML) coated QDs, which is described by a modification of eq 3 as

$$I_{PL}(T) = \frac{N_0 + N'_0 e^{-\Delta E/k_B T}}{1 + B(e^{E_{LO}/k_B T} - 1)^{-m}} \quad (4)$$

where ΔE is the potential depth of these localized trap states, N'_0 is a parameter that is related to the density of trap states. The parameters m and ΔE for CdSe/CdS (6 ML) and CdSe/multishell (6 ML) are also summarized in Table 2. Compared with the experimental data in Figure 4, the nonradiative

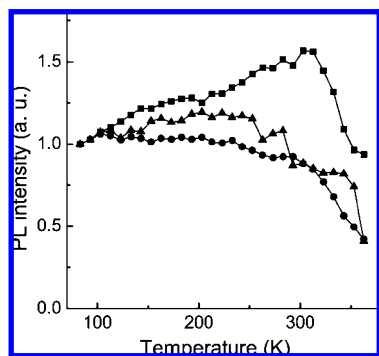


Figure 5. Temperature dependence of integrated PL intensity for CdSe core/multishell QDs before (squares) and after heavy washing (triangles). The circles represent that of the blend of the QDs and TPD.

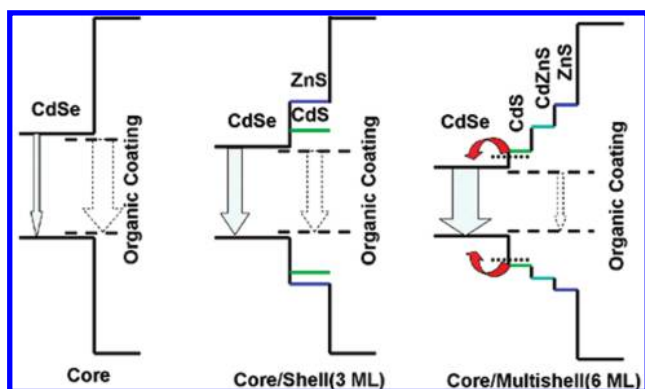


Figure 6. Schematic diagrams of electronic levels of CdSe core, CdSe/CdS, or ZnS core/monoshell (3 ML) and CdSe/CdS/CdZnS/ZnS core/multishell (6 ML) QDs. Dashed arrowheads show the nonradiative recombination processes. Dashed lines show the nonradiative recombination centers formed on the surface or at the interface of the QDs. Red arrowheads show the thermal activation of localized carriers.

recombination rate in CdSe/CdS (6 ML) QDs is larger than that in CdSe core/multishell (6 ML) QDs. Therefore, the outer layer with a high band offset in the core/multishell QDs can effectively confine the electron and the hole into the core, resulting in high QY of the QDs with a multishell.¹³

In order to understand the ligand shell effect on the PL property, the temperature-dependent PL spectra of CdSe core/multishell QDs with different surface treatment were studied as shown in Figure 5. The PL QY of the QDs was significantly dropped from 70% to 30% before and after heavy washing. It is found that the enhancement of the PL intensity with increasing temperature almost disappears. This means that the removal of the ligands on the surface of the QDs results in formation of a large amount of surface dangling bonds, quenching the PL.^{13,34} In addition, the temperature-dependent PL spectra of CdSe core/multishell QDs in an HTM matrix, *N,N'*-diphenyl-*N,N'*-bis(3-methylphenyl)-1,1'-biphenyl-4,4'-diamine (TPD) are shown in Figure 5. Similarly, the PL enhancement with increasing temperature was not observed. The PL quenching of the QDs was observed due to the removal of emitting centers at the surface of core/shell QDs and hole transfer from the QDs to the HTMs.¹⁴

We also studied temperature-dependent PL spectra of CdSe core/shell QDs, such as CdSe/CdZnS (6 ML), CdSe/CdS (3 ML)/ZnS (3 ML), and CdSe/CdS (2 ML)/CdZnS (2 ML)/ZnS (2 ML) and obtained similar experimental results (see Figures S1, S2, and S3, Supporting Information). Figure 6 shows schematic diagram of electronic levels and structures of the CdSe core, core/monoshell and core/multishell QDs, and the highest

occupied molecular orbital (HOMO) and the lowest unoccupied molecular orbital (LUMO) levels of the organic ligands. Therefore, the improvement mechanism of the PL QY in the CdSe core/multishell QDs can be understood well in terms of the effective passivation of the following nonradiative pathways: (i) a monoshell such as ZnS and CdS can effectively reduce defects/traps on the core surface, but a large amount of interface traps (dislocation) forms at the interface between the CdSe core and the ZnS shell with increasing the shell thickness,^{13,15} as well as the low conduction band offset between the CdSe core and CdS shell can not effectively confine the electron in the core;¹⁴ (ii) a multishell can perfectly passivate defects/traps on the core surface and at various interfaces due to a small lattice mismatch between the CdSe core and CdS, CdZnS, and ZnS shells;¹³ and (iii) ligands at the surface of the QDs clearly reduce the density of the nonradiative recombination centers on an outer ZnS shell.

Conclusions

In summary, we have studied the temperature-dependent PL spectra of CdSe core/shell QDs with different shell structures (ZnS, CdS, and CdS/CdZnS/ZnS). The evolution of temperature-dependent nonradiative relaxation processes is clearly demonstrated from thermal activation of carrier trapping by surface defect states in the core QDs to the thermal escape of carriers from the core in the core/shell QDs. The nonradiative recombination on the surface and at the interfaces can be dramatically suppressed by a multishell structure with the appropriate thickness due to a small lattice mismatch between the layers. In particular, the enhancement of PL intensity observed in the core/multishell QDs with increasing temperature from 80 to 300 K is well explained in terms of delocalization of the carriers localized at the core(CdSe)/shell(CdS) interface states induced by atom diffusion or lattice strain. Furthermore, the carriers can also be effectively captured by surface dangling bonds or attached HTMs despite a thick multishell on the core QDs. The experimental results clearly indicate the shells play an important role in reducing the nonradiative relaxation processes in the core/shell QDs. It will be surely promising to design the shell structure to control PL properties of the QDs for improving the performance of QD-based devices.

Acknowledgment. This work was supported by the program of CAS Hundred Talents, NSF of China (10874179, 10874180, 10674132, and 60771051), and Pre-Strategic Initiative of University of Tsukuba, Japan.

Supporting Information Available: Temperature dependence of emission peak energy, fwhm, and PL intensity for CdSe/CdZnS (6 ML) (size, 7.0 nm), CdSe/CdS (3 ML)/ZnS (3 ML) (size, 7.0 nm), and CdSe/CdS (2 ML)/CdZnS (2 ML)/ZnS (2 ML) (size, 5.0 nm) core/shell QDs. This material is available free of charge via the Internet at <http://pubs.acs.org>.

References and Notes

- (1) Colvin, V. L.; Schlamp, M. C.; Alivisatos, A. P. *Nature* **1994**, *370*, 354.
- (2) Coe, S.; Woo, W. K.; Bawendi, M.; Bulovic, V. *Nature* **2002**, *420*, 800.
- (3) Zhao, J. L.; Bardecker, J. A.; Munro, A. M.; Liu, M. S.; Niu, Y. H.; Ding, I. K.; Luo, J. D.; Chen, B. Q.; Jen, A. K.-Y.; Ginge, D. S. *Nano Lett.* **2006**, *6*, 463.
- (4) Niu, Y. H.; Munro, A. M.; Cheng, Y. J.; Tian, Y. Q.; Liu, M. S.; Zhao, J. L.; Bardecker, J. A.; Plante, I. J.; Ginger, D. S.; Jen, A. K.-Y. *Adv. Mater.* **2007**, *19*, 3371.
- (5) Sun, Q. J.; Wang, Y. A.; Li, S. L.; Wang, D. Y.; Zhu, T.; Xu, J.; Yang, C. H.; Li, Y. F. *Nature Photon.* **2007**, *1*, 717.

- (6) Jing, P. T.; Zheng, J. J.; Zeng, Q. H.; Zhang, Y. L.; Liu, X. M.; Liu, X. Y.; Kong, X. G.; Zhao, J. L. *J. Appl. Phys.* **2009**, *105*, 044313.
- (7) Schlamp, M. C.; Peng, X. G.; Alivisatos, A. P. *J. Appl. Phys.* **1997**, *82*, 5837.
- (8) Mattoussi, H.; Radzilowski, L. H.; Dabbousi, B. O.; Thomas, E. L.; Bawendi, M. G.; Rubner, M. F. *J. Appl. Phys.* **1998**, *83*, 7965.
- (9) Huynh, W. U.; Dittmer, J. J.; Alivisatos, A. P. *Science* **2002**, *295*, 2425.
- (10) Sun, B. Q.; Marx, E.; Greenham, N. C. *Nano Lett.* **2003**, *3*, 961.
- (11) Bruchez, M.; Moronne, M.; Gin, P.; Weiss, S.; Alivisatos, A. P. *Science* **1998**, *281*, 2013.
- (12) Dabbousi, B. O.; Rodriguez-Viejo, J.; Mikulec, F. V.; Heine, J. R.; Mattoussi, H.; Ober, R.; Jensen, K. F.; Bawendi, M. G. *J. Phys. Chem. B* **1997**, *101*, 9463.
- (13) Xie, R.; Kolb, U.; Li, J.; Basche, T.; Mews, A. *J. Am. Chem. Soc.* **2005**, *127*, 7480.
- (14) Zhang, Y. L.; Jing, P. T.; Zeng, Q. H.; Sun, Y. J.; Su, H. P.; Wang, Y.; Andrew, Kong, X. G.; Zhao, J. L.; Zhang, H. *J. Phys. Chem. C* **2009**, *113*, 1886.
- (15) Cretí, A.; Anni, M.; Rossi, M. Z.; Lanzani, G.; Leo, G.; Sala, F. D.; Manna, L.; Lomascolo, M. *Phys. Rev. B* **2005**, *72*, 125346.
- (16) Valerini, D.; Cretí, A.; Lomascolo, M.; Manna, L.; Cingolani, R.; Anni, M. *Phys. Rev. B* **2005**, *71*, 235409.
- (17) Morello, G.; De Giorgi, M.; Kudera, S.; Manna, L.; Cingolani, R.; Anni, M. *J. Phys. Chem. C* **2007**, *111*, 5846.
- (18) Al Salman, A.; Tortschanoff, A.; Mohamed, M. B.; Tonti, D.; van Mourik, F.; Chergui, M. *Appl. Phys. Lett.* **2007**, *90*, 093104.
- (19) Wuister, S. F.; van Houselt, A.; de Mello Donegá, C.; Vanmaekelbergh, D.; Meijerink, A. *Angew. Chem., Int. Ed.* **2004**, *43*, 3029.
- (20) Peng, Z. A.; Peng, X. G. *J. Am. Chem. Soc.* **2001**, *123*, 183.
- (21) Babentsov, V.; Riegler, J.; Schneider, J.; Ehlert, O.; Nann, T.; Fiederle, M. *J. Cryst. Growth* **2005**, *280*, 502.
- (22) Ramvall, P.; Tanaka, S.; Nornura, S.; Rblet, P. *Appl. Phys. Lett.* **1999**, *75*, 1935.
- (23) Wan, J. Z.; Brebner, J. L.; Leonelli, R.; Zhao, G.; Graham, J. T. *Phys. Rev. B* **1993**, *48*, 5197.
- (24) Lee, J.; Koteles, E. S.; Vassell, M. O. *Phys. Rev. B* **1986**, *33*, 5512.
- (25) Baranov, A. V.; Rakovich, Yu. P.; Donegan, J. F.; Perova, T. S.; Moore, R. A.; Talapin, D. V.; Rogach, A. L.; Masumoto, Y.; Nabiev, I. *Phys. Rev. B* **2003**, *68*, 165306.
- (26) Lange, H.; Artemyev, M.; Woggon, U.; Niermann, T.; Thomsen, C. *Phys. Rev. B* **2008**, *77*, 193303.
- (27) Takagahara, T. *Phys. Rev. Lett.* **1993**, *71*, 3577.
- (28) Schnitt-Rink, S.; Miller, D. A. B.; Chemla, D. S. *Phys. Rev. B* **1987**, *35*, 8113.
- (29) Klimov, V.; Bolivar, P. H.; Kurz, H. *Phys. Rev. B* **1996**, *53*, 1463.
- (30) Yang, W.; Lowe-Webb, R. R.; Lee, H.; Sercel, P. C. *Phys. Rev. B* **1997**, *56*, 13314.
- (31) Efros, A. L.; Rosen, M. *Phys. Rev. B* **1998**, *58*, 7120.
- (32) Meulenber, R. W.; Lee, J. R. I.; Wolcott, A.; Zhang, Jin Z.; Terminello, L. J.; van Buuren, T. *ACS Nano* **2009**, *3*, 325.
- (33) Gindele, F.; Hild, K.; Langbein, W.; Woggon, U. *Phys. Rev. B* **1999**, *60*, 2157.
- (34) Chen, Y. F.; Vela, J.; Htoon, H.; Casson, J. L.; Werder, D. J.; Bussian, D. A.; Klimov, V. I.; Hollingsworth, J. A. *J. Am. Chem. Soc.* **2008**, *130*, 5026.
- (35) Zhagan, V. M. D.; Valakh, M. Y.; Raevskaya, A. E.; Stroyuk, A. L.; Kuchmiy, S. Y.; Zahn, D. R. T. *Nanotechnology* **2007**, *18*, 285701.
- (36) Kanie, H.; Sugimoto, K.; Okado, H. *Mater. Res. Soc. Symp. Proc.* **2001**, *639*, 6184.
- (37) Han, T. T.; Fu, Y.; Wu, J.; Yue, Y.; Dai, N. *J. Phys. D: Appl. Phys.* **2008**, *41*, 115104.
- (38) Smith, A. M.; Mohs, A. M.; Nie, S. M. *Nat. Nanotechnol.* **2009**, *4*, 56.
- (39) Ithurria, S.; Guyot-Sionnest, P.; Mahler, B.; Dubertret, B. *Phys. Rev. Lett.* **2007**, *99*, 265501.
- (40) Wong, P. S.; Liang, B. L.; Dorogan, V. G.; Albrecht, A. R.; Tatebayashi, J.; He, X.; Nuntawong, N.; Mazur, Y. I.; Salamo, G. J.; Brueck, S. R. J.; Huffaker, D. L. *Nanotechnology* **2008**, *19*, 435710.
- (41) Mu, X. D.; Ding, Y. J.; Ooi, B. S.; Hopkinson, M. *Appl. Phys. Lett.* **2006**, *89*, 181924.
- (42) Jones, M.; Lo, S. S.; Scholes, G. D. *Proc. Natl. Acad. Sci. U.S.A.* **2009**, *106*, 3011.